Design and Testing of a Frequency Selective Surface (FSS) Based Wide-Band Multiple Antenna System

A Thesis

Presented in Partial Fulfillment of the Requirements for the Degree of Bachelor of Science with Distinction in the College of Engineering and the University Honors Program

By
Dana C. Kohlgraf
*****
Department of Electrical and Computer Engineering
The Ohio State University
2005

B.S. Committee:
Dr. Eric K. Walton, Co-advisor
Dr. Roberto G. Rojas, Co-advisor

Abstract

Since the first radio link was built by Hertz in 1886, antennas have become a critical technology which allows people to stay connected and informed. Several advances have been made in the field of antenna theory and technology in the past hundred twenty years. Among them is the characterization of frequency selective surfaces (FSS), which are periodic arrays of passive elements or slots that act as a band stop or a band pass filters respectively to propagating electromagnetic waves.

The purpose of this project was to construct an antenna which is transmissive outside of the band of operation. For example, the antenna designed in this project operates in a band of 1-2 GHz. The goal of this project is to be able to place an antenna operating at 4-8 GHz behind this antenna and have it be able to "look though" the first antenna as if it wasn't there. This will allow the user to stack antennas one behind the other and thus increase the density of antennas in a given area. This is advantageous in applications where the available real estate upon which to place antennas is limited, such as on ships and submarines.

This antenna has two main components - an array of radiating elements and a reflector. The radiating array will be transmissive at 4-8 GHz as long as it does not radiate energy at this frequency and does not significantly scatter energy. These constraints are easily met by creating an array of wire elements. Reflectors, on the other hand, are commonly composed of a solid metal plate, which will reflect energy at any frequency. However, this project uses an element FSS for a reflector. As a result this reflector will only reflect energy in the stop band. Sufficiently outside of this band, it

will be transmissive. While an entire antenna was designed for sake of completeness, the focus of this project was the design and testing of the FSS reflector.

There were two main components to this project. The first was to use computational codes to design the antenna. Specifically, the antenna was designed using a Method of Moments (MoM) code, which calculates gain patterns for finite antennas. These results were then compared to a periodic moment method code, which calculates the ideal result for an infinite structure. This design process was completed in several steps. First the FSS array was designed to be reflective in the L band (1-2 GHz) and transmissive outside of this band. Following this the radiating array was designed to realize sufficiently flat L band bandwidth. The FSS reflector and radiating array were then combined together and the gain and transmissivity were then calculated for the entire antenna. Finally a prototype of the FSS reflector was built and tested. Time constraints prevented the construction of the entire antenna.

The results of these tests are in very good agreement with each other. MoM tests show the FSS is within 1 dB of perfect reflectivity over the entire L band range. The prototype was within 2 dB of perfect reflectivity over the same range. This deviation is explained by unavoidable human error in the construction of the FSS. The periodic moment method code is also computed similar results. The bandwidth wasn't quite as large in the PMM test, but this is expected and is explained by the fact that edge diffraction on finite structures increases the bandwidth. The transmissivity of this FSS is within 2 dB of perfect transmissivity in the C band (4-8 GHz.) Finally the gain of the radiating array has a 2 dB variation over L band, and the gain of the entire antenna has a 3 dB variation over L band.

Table of Contents

Page

Lists of Figures

Figure **Page**

List of Tables

Table **Page**

Lists of Symbols

λ	wavelength (m)
λ_0	design wavelength (m)
λ_{1425}	wavelength at 1425 MHz (m)
D	distance (m)
ε_r	relative permittivity (F/m)
ε_{eff}	effective permittivity (F/m)

Chapter 1

Introduction

1.1 Background

Since radio transmission was first demonstrated by Heinrich Hertz at the Technical Institute in Karlsruhe, Germany in 1886 and Guglielmo Marconni's success with transatlantic communication in the beginning of the 20th century, antennas have become an indispensable technology, linking people and places in ways that people could only dream of a century ago [1]. Antennas have permeated into many aspects of our daily lives, and have enabled several advances in mankind's knowledge of both Earth and its inhabitants and the universe in which we live.

A wide variety of antennas are utilized for an array of applications, from weather and global positioning satellites to ground based antenna arrays which are used to receive extraterrestrial radio transmissions to antennas used in radios and cell phones. A

multitude of antenna types exist, including monopole and dipole antennas, loop antennas, dish antennas, and horn antennas. These antennas can be arranged in arrays to realize high gain and directivity with several small antennas instead of one large antenna.

One type of array is known as a Frequency Selective Surface (FSS). This array can be either radiating or non-radiating and is composed of a periodic array of elements or slots. Element and slot FSS arrays effectively create band stop and band pass filters respectively to electromagnetic energy at their design frequency range. These types of filters are used in a wide variety of applications, including radomes, dichroic surfaces, circuit analog absorbers and meanderline polarizers [1].

Radomes are the protective cover placed in front of an antenna. For applications, such as military aircraft, these surfaces are designed such that the radar cross section (RCS) of a structure is minimized. Circuit analog absorbers are composed of a periodic array of resistive elements which when designed properly can achieve greater than 25 dB of attenuation over a decade of bandwidth (frequency ratio of 10:1.) Meanderline polarizers are used to transform linear polarization to circular polarization and vice versa over a bandwidth of up to an octave (frequency ratio of 2:1) [1].

Finally a dichroic surface is one which is designed to be reflective at one frequency and transmissive at another. One application of dichroic surfaces is creating a combination single/dual reflector system [1]. In this design, the main reflector, which is the largest and heaviest part of an antenna, is used to operate the main reflector in conjunction with an FSS subreflector at one frequency and as the only reflector at another frequency. The subreflector is designed to be transmissive at the band the second feed operates at so that the single reflector system performance will not be significantly

degraded by the presence of the subreflector [1]. This design allows two antennas to be effectively placed in the space of one, which, in addition to the fact that less 'hardware' is needed, allows for significant cost and space savings.

The purpose of this project was to design an antenna roughly similar to a dichroic surface. Instead of designing a combination single/dual reflector system, though, this project's goal was to design an antenna which is transmissive outside of the band of operation. For this project, an antenna composed of an array of wide-band radiating elements over a wide-band FSS reflector was designed. For practical reasons, this antenna was designed to operate in the L-band (1-2 GHz.) This antenna was designed using an industry standard Moment of Methods (MoM) code known as ESP5, which was developed at the ElectroScience Lab. A prototype of this design was then constructed and tested. More details on this antenna can be found in chapter 3.

1.2 Rationale

The major reason for pursuing this project is that while the number of applications for antennas has been increasing over time, the available real estate upon which to place these antennas has not necessarily been keeping pace. For some industries where available real estate is limited, such as aircraft and naval vessels, there is naturally a great deal of interest in being able to fit more antennas into a given area.

Since

$$Gain \propto \frac{Aperture_{effective}}{\lambda^2}$$

a simple scaling of existent antennas comes at the cost of reduced gain for a given frequency [1]. The frequency is operation is more or less fixed by the application and

gain must be high enough to maintain a sufficient signal to noise ratio (S/N); as a result it is not always possible to simply scale antennas down in order to pack more in to a given area. One possible alternative is to pack antennas into a closer area. Since an obstructed field of view also diminishes the antenna gain by scattering the signal, it is necessary for antennas in front to be relatively transparent to antennas "looking through" them.

For this project, a wide-band antenna has been designed. There are several reasons to design a wide-band instead of narrow-band antenna. The first is the fact that wide-band arrays are inherently more difficult to design. As such, once the design of wide-band arrays has been mastered, it is relatively simple to apply that knowledge to the design of narrow-band arrays. In addition, wide-band arrays present several advantages over narrow-band arrays. First, the wider the bandwidth, the more channels of a given bandwidth can be simultaneously transmitted or received. This is especially important for applications which operate over a range of frequencies.

This antenna is designed to operate in the L-band. This band was chosen mostly a matter of practicality. Specifically, an antenna designed at this frequency is composed of elements which are large enough to be reliably constructed by hand yet small enough that the array is a manageable size. Since gain is proportional to the effective aperture over the wavelength squared, an antenna designed at one frequency can be simply scaled up or down to another frequency and realize the same gain pattern at another frequency.

1.3 Overview of Necessary Definitions

The typical definition of a wide-band antenna is an antenna whose 3 dB beamwidth is at least an octave, in other words the highest frequency of operation is twice the lowest

frequency of operation. This is the definition which will be used for this project. Ideally the antenna gain would be perfectly flat and the FSS reflector would be perfectly reflective over the entire range of operation; however as long as the radiating array gain is stable over the range of operation, the FSS reflectivity is within 1-2 dB of perfect reflectivity over the entire range of operation and the radiating array does not couple too strongly to the FSS, the antenna will perform sufficiently well.

Chapter 2

Theory

2.1 Introduction

This section will provide the necessarily FSS and radiating array antenna theory necessary to understand and design this wide-band antenna array, with particular attention paid to the design of the FSS reflector. FSS theory will be built starting with a comparison of available elements. Afterwards infinite (ideal) arrays and finite (actually realizable) arrays will be discussed. Finally this section ends with a discussion of wide-band radiating arrays.

2.2 Frequency Selective Surface (FSS) Theory

2.2.1 Introduction

As was noted earlier, a frequency selective surface is a periodic array of either radiating or non-radiating elements or slots which effectively act as a band stop or band pass filter

respectively to electromagnetic waves. There are a wide variety of possible elements which can be used to realize FSS arrays as will be discussed in later in this section.

This section on FSS theory will proceed in a similar manner as the earlier basic antenna theory. Different types of possible FSS elements will be discussed first, followed by infinite array theory, where much of the FSS groundwork will be laid out, and finally finite array theory, where additional considerations when dealing with finite arrays are discussed.

2.2.2 FSS Element Comparison

There are four different types of possible element-type FSS arrays: center connected, loop, plate and combination. See Figure 2.1 for some examples of each element type [2]. Each group of elements is ordered from most narrow-banded on the left to most wide-banded on the right. Each type will be discussed in more detail in the following paragraphs. In addition to the above element groups, the rough compliment of these elements may be realized by cutting slots in a plate. Discussion of slot FSS arrays is beyond the scope of this paper. Consult, for example, [2] for a detailed discussion on the design and application of slot arrays. It is, however, important to note that slots and elements are not prefect inverses of each other. One cannot design a band stop filter with elements and convert it to an identical slot configuration and expect to get an opposite but otherwise identical band pass filter [2].

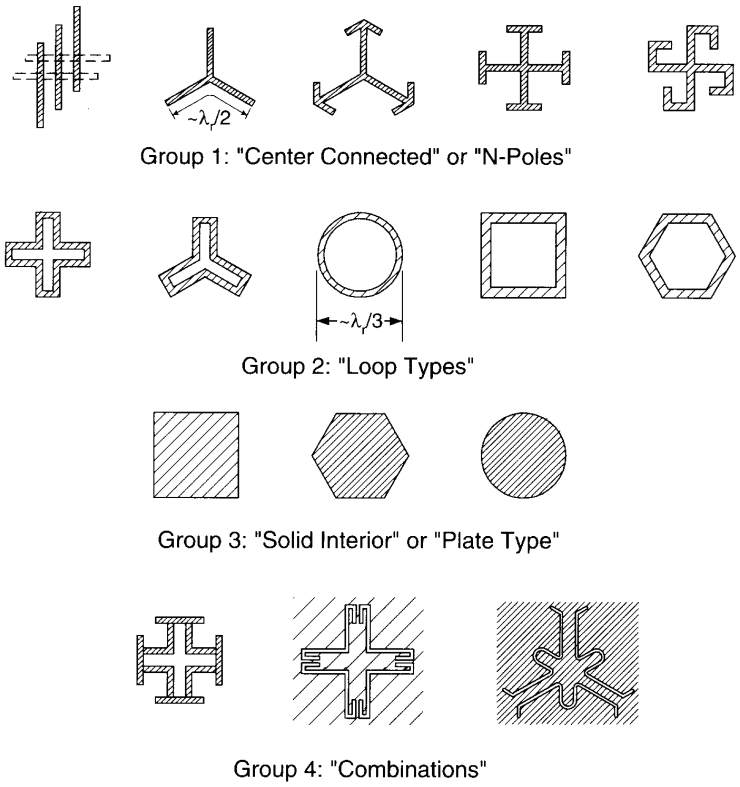

Figure 2.1: The four major groups of FSS elements. These elements may be used to construct band stop filter type FSS arrays. Elements are ordered from most narrow-banded on the left to most wide-banded on the right. From [2].

The first group, the center connected elements, are a viable candidate for both radiating and non-radiating arrays. Perhaps the most recognizable from the center connected group is the dipole [2]. This is by nature a narrow banded element, but when placed in a well designed array this element is capable of reaching a ratio of 4:1 without the addition of a dielectric matching section added in front of the array of a bandwidth or a decade or better with a dielectric matching section [3]. This is mentioned to demonstrate that the bandwidth of an individual element does not necessarily determine the bandwidth of the array. However, element bandwidth does provide a good starting point for designing wide-band arrays. The details of how to obtain larger bandwidths is described later in this section.

The loop elements are in general an excellent choice for non-radiating element FSS arrays. These elements are typically smaller in the x and y directions than the center connected elements with respect to a wavelength and thus can be spaced close to one another. As will be discussed in more detail later, this leads to delayed onset of grating lobes and generally wider bandwidth [2].

Perhaps the most notable of the loop elements for the purpose of this paper is the hexagon loop, which not only has superior wide-band element performance but also can be stacked close together to achieve extremely wide-band array performance. The reason for this behavior can be easily explained by looking at a column of hexagonal elements, like the one shown in top of the left column in Figure 2.2. The four side wires of each element are inductive in nature and capacitors are formed between the top and bottom wire segments of adjacent elements. This leads to the equivalent circuit shown at the bottom of the left column in Figure 2.2 [2].

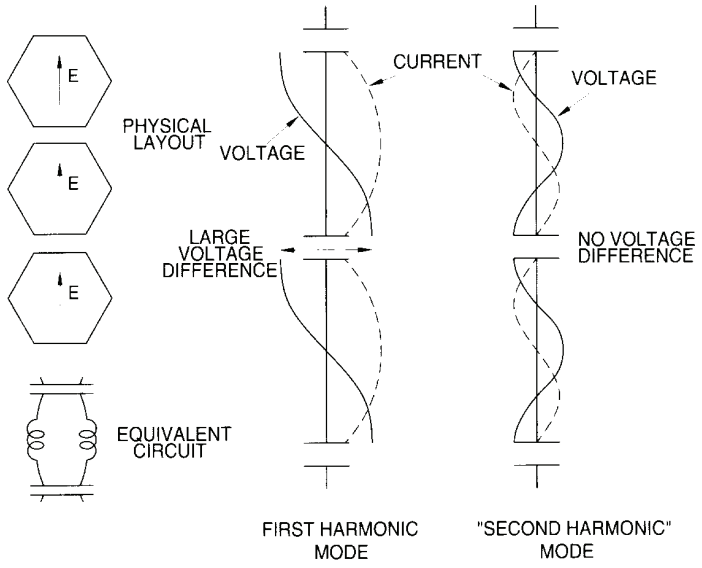

Figure 2.2: Figure explaining why the hexagonal element has superior wide-band characteristics. The left column shows a column of hexagonal elements on top and the equivalent circuit for this array bottom. Each element has four side wires which contribute to the inductance and the top and bottom wires of adjacent elements form capacitors. The middle and right columns show the current and voltage distributions of the first two harmonic modes. Notice that there is a large voltage difference across the capacitor in the first harmonic mode but not in the second. This large voltage difference causes a much a capacitance between the wires which drives the resonance down in frequency. This results in a large bandwidth. From [2].

The presence of the capacitors forces the current distribution to go to zero at the top and bottom wires. The first harmonic mode is thus formed when the current distribution forms a half wavelength sinusoid between capacitors. This current distribution results in the voltage and distribution shown in the center column of Figure 2.2 [2]. This results in a large voltage difference across the capacitors, which in turn drives the first resonance down in frequency. The second harmonic mode occurs when the current forms a full sinusoid. The voltage distribution for this mode is shown in the right most portion of Figure 2.2. As this figure shows, there is no voltage difference across the capacitors meaning the frequency of the second resonance will not be pulled down [2].

This behavior is not the case for most elements. For example the anchor element, which is the middle element in group 1 in Figure 2.1, has the current and voltage distributions shown in Figure 2.3 for the first two harmonic modes. Notice that the capacitance occurring between the center of one element and the end of another element has a large voltage distribution across it. Thus both resonances are pulled significantly downward [2].

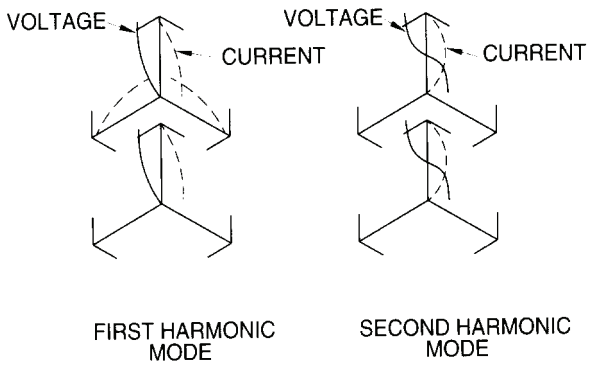

Figure 2.3: Voltage and current distributions for a tripole element. Notice that there is a voltage difference across the capacitors, which extends from the tip of one element to the leg of another, for both harmonic modes. Thus both modes are pulled down significantly in frequency. From [2].

Plate elements in general do not have very desirable characteristics. First the element have x and y dimensions around a half of a wavelength, which limits how closely these elements can be placed next to one another. In addition plates are highly inductive elements with small capacitances between them, leading to issues with regard to achieving resonance. If the FSS never resonates, then it is impossible to achieve perfect reflection. This is due to the fact that at resonance, the FSS becomes a short circuit (assuming the materials are lossless) and thus acts as a perfect electric conductor (PEC) ground plane [2].

Finally combination elements are too diverse to generalize in any meaningful way. The possibilities in this group are as boundless as the imagination of the designer. Some possible examples of elements in this group have already been shown in Figure 2.1 [2].

2.2.3 Infinite FSS Arrays

The purpose of this section is to discuss several considerations when designing an FSS array. Due to periodicity requirements, the only true FSS is an infinite one. It is thus quite instructive to discuss the properties of infinite FSS arrays and apply this knowledge to the closest realizable approximation, namely finite FSS arrays. This section is followed by a section on finite FSS arrays since making an array finite complicates the picture. For example, it is possible to excite radiating surface waves on finite FSS arrays, but not on infinite FSS arrays. This will be discussed in more detail in the next section.

Techniques to Increase Bandwidth

The first major consideration when designing an FSS is bandwidth. The previous section alluded to the fact that closer element spacing leads to larger bandwidth. This can be most easily explained by remembering that the FSS will act as reasonably good ground plane when the impedance is very low. One way to achieve low impedance is to have all the capacitive components of the FSS more-or-less cancel all of the inductive components. Another method is to simply minimize the total possible impedance.

The increase in bandwidth when the element spacing is reduced can be explained indirectly by the fact that an element in an array has a lower impedance than the same element isolated in free space. This can be conceptually explained by the fact that while

a single element has the ability to store charge between the edge of the element to infinity, this same element placed in an array is only able to store charge from the edge of the element to half the distance to its nearest neighbor. This reduces the volume within which charge may be stored, which in turn reduces the stored charge [3]. A good rule of thumb is that a 10 percent reduction in the inter-element spacing in either direction will result in about a 10 percent increase in bandwidth, and a 10 percent reduction in inter-element spacing in both directions will result in about a 20 percent increase in bandwidth.

For most elements, this change in inter-element spacing does not significantly change the resonant frequency. Elements with high end capacitance such as closely spaced dipole elements or hexagon elements, however, will see such a large increase in capacitance that the resonant frequency as the inter element spacing is decreased. This will cause the resonate frequency to be driven downward. For these elements the resonant frequency can be shifted to lower frequencies by increasing the element size for a given element spacing and to higher frequencies by decreasing the element size for a given element spacing [2].

Another way to increase the bandwidth is to use fatter wires. This increases the bandwidth by reducing the inductance of the wires. If the wire radius is increased too much, however, the inductance will be reduced to the point where it will never cancel the capacitance (the surface will never resonate) [3].

The bandwidth of an FSS can also be dramatically increased by stacking two identical FSS arrays, one in front of the other. Whereas a single FSS will typically only have one frequency with perfect reflection, stacking two identical FSS arrays causes the

bandwidth to maintain nearly perfect reflection over a wide range of frequencies and causes the reflectivity to fall off sharply at the stop band edges [2].

When these two arrays are cascaded, three distinct array interference notches materialize, at a low, middle and high frequency, f_L, f_M, f_H. The reason for these three nulls is explained by looking at the equivalent circuit model representation of the two FSS arrays. A circuit model is shown in top left corner of Figure 2.4 [2]. By plotting the admittance of the array on the Smith chart, it becomes clear why these nulls form.

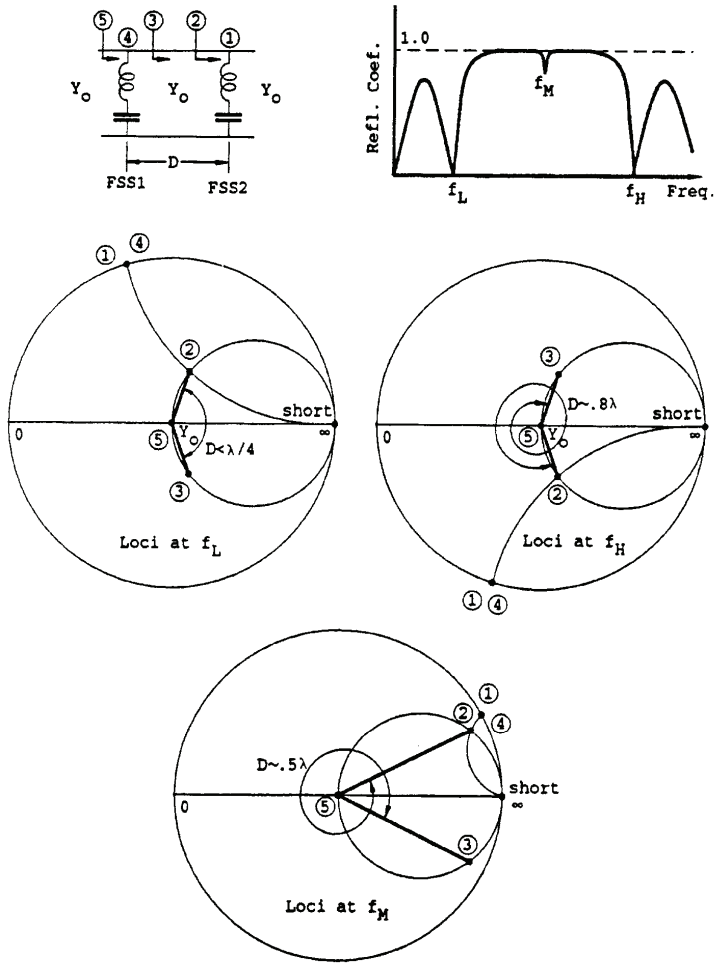

Figure 2.4: Admittance plots showing the reason for the three array interference nulls that form when two identical FSS are cascaded, one in front of the other. These plots show that array interference nulls occur when the reactive part of the impedance to the right of the left FSS is equal to the reactive part of the FSS. From [2].

The Smith charts in this graph show the admittance plots at each of the three array interference nulls. The first interference null is shown in the top left Smith chart and occurs when $D<\lambda/4$ at a particular 'design' frequency. The Smith chart for the upper frequency null is shown in the top right figure; this null occurs when $D\sim0.8\lambda$. Finally the Smith chart at the bottom of the figure shows the middle interference null. This null occurs when $D\sim0.5\lambda$ at a particular 'design' frequency [2].

These admittance plots are found by starting with the free space admittance to the right of the FSS arrays. Added to this is the admittance of the rightmost FSS, which is represented by an LC circuit (1) to obtain the total admittance (2). This admittance is then rotated a distance of D/λ, where D is the spacing between the arrays (3). The admittance from FSS 1 (4) is added to (3) to obtain (5). If the admittance in (3) and (4) are the same but with opposite signs, the sum (5) will go through the center of the Smith chart, which corresponds to zero reflection, resulting in an array interference null [2].

The null at f_M will disappear (or become infinitely thin) if both of the FSS arrays are resonant at f_M. This occurs when the spacing, $D=\lambda_0/2$. The $D=\lambda/2$ spacing shown in the bottom of Figure 2.4 is for a 'design' frequency below the resonant frequency. Since this null typically occurs at the middle of the band, this spacing is a rather rigid design constraint. Cascading two identical FSS arrays results in a reflection curve with a much flatter top and a faster roll off compared to a single FSS array [2].

If cascading two identical FSS arrays does not provide sufficient bandwidth, the designer can add a third FSS which is resonant at the upper null. It is also possible to cascade two FSS arrays which are not identical. This second suggestions is not

recommended since the upper and lower nulls will be filled in and a distinct null will form around the middle frequency [2].

While the designer could in theory cascade several FSS arrays, this significantly adds to the bulk and should not be necessary if the FSS has been designed well [2]. Even two dipole arrays which have been well designed are capable of achieving a bandwidth of 4:1 [3]. For the sake of argument, the rest of the theory discussion will employ an FSS consisting of two identical FSS arrays separated by a distance of $0.5\lambda_0$.

Methods to Improve Transmissivity Outside of the Stop Band

In addition to designing the FSS to be reflective in the design band, it is important for the FSS to be transmissive outside of this band so that another antenna is able to "look though" it. There are a couple of techniques which can be used to improve the transmissivity outside of the design band, which are discussed in the next two paragraphs.

The easiest way to improve the transmissivity outside of the design band is to reduce the bandwidth of the design band. The reason for this can be seen by looking at Figure 2.5. This figure shows the equivalent circuit for two cascaded FSS arrays in the top of the figure for easy reference. The Smith chart admittance plots are found by the same analysis used for Figure 2.4. The two Smith charts on the left hand side shows the admittance between f=0 to f=f_L for an FSS system with a certain bandwidth. To reduce clutter, the final admittances (5) are shown on a separate Smith chart [2].

The two Smith charts to the right show the same plots for a system of two cascaded FSS arrays which have a smaller bandwidth. Note that the spacing between the arrays for each case was adjusted so that the null at f_M disappears. As can be seen,

lowering the bandwidth also causes f_L to shift down in frequency. This in turn reduces the admittance mismatch between (3) and (4) between f=0 and f= f_L. Thus the transmissivity improves over this range, as is shown by the bottom two plots in Figure 2.5 [2]. Since there is a tradeoff between bandwidth and transmissivity, it is desirable to design the FSS array such that the bandwidth requirements are met but not significantly exceeded.

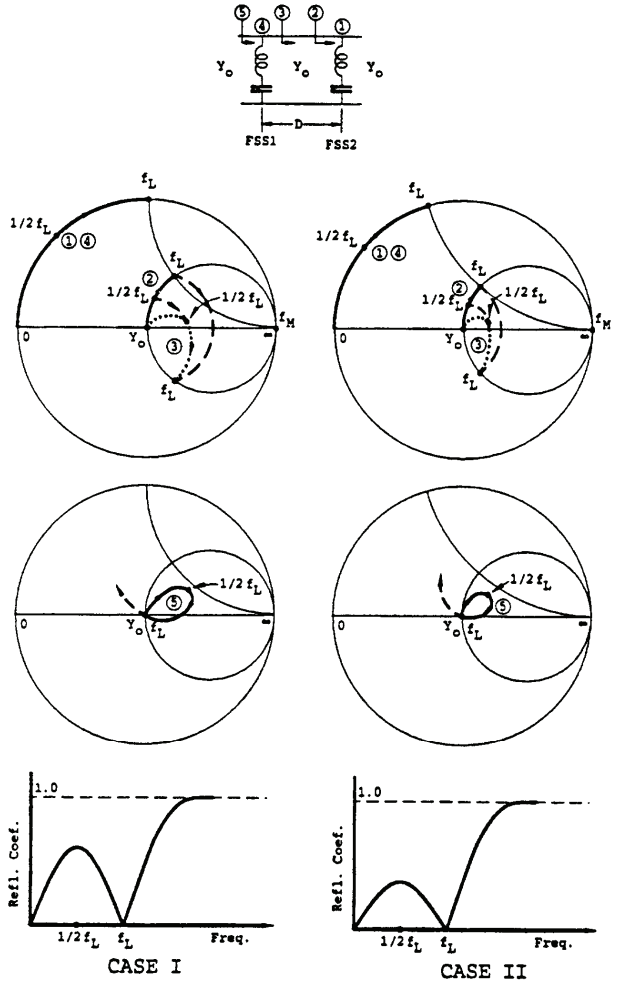

Figure 2.5: This figure shows that the transmissivity outside of the design band is improved when the bandwidth of the FSS is reduced. From [2].

A second way to improve the transmissivity is to add dielectric matching section in front of and behind the FSS. This matching section, like in transmission line theory, will act to reduce the reflections between the FSS array and free space by bringing the array impedance close to the center of the Smith chart over a wide range of frequencies [2]. Since dielectrics were not added to this design, discussion of this topic is beyond the scope of this paper. See [2] for a discussion of the pertinent theory.

Grating Lobes

A final important consideration when designing an FSS array is the onset of grating lobes. Rays from two different collinear point sources are delayed in phase by

$$\Psi = r\sin(\theta)\cos(\phi)$$

If this phase delay is equal to 2π, the two sources will add in phase and create a grating lobe. The smallest spacing this will occur when

$$\sin(\theta)\cos(\phi) = 1$$

or in other words when

$$r_{rad} = \frac{2\pi r_m}{\lambda} = 2\pi$$

thus when

$$r_m = \lambda$$

However if the element does not radiate energy in the direction of a grating lobe, then the lobe can not radiate energy. This is easily shown by considering that an array pattern can be generated using pattern multiplication, which states that

$$E(\theta,\phi) = E_s(\theta,\phi)E_x(\theta,\phi)E_y(\theta,\phi)E_z(\theta,\phi)$$

where E_s is the pattern of a single element, and E_x, E_y and E_z are the patterns of a linear array of point sources in the x, y and z directions respectively [1]. Thus, if the source doesn't radiate energy in a given direction, then neither will the array.

The presence of grating lobes for many applications has the potential to significantly degrade the performance of an antenna. For example if an antenna is being used as a receive antenna, it will receive signals from both the desired direction and also the direction in which the grating lobe is present. Since this project will use elements which are spaced close together to achieve a higher bandwidth, this will only potentially become a problem at very high frequencies, where the FSS should be transmissive. Since grating lobes are only a function of frequency and element spacing, it is not possible to avoid grating lobes forever. It is mostly important to be aware of their presence.

Estimation of Resonant Frequency and Effect of Dielectric Substrates

When designing an FSS, it is very helpful to be able to estimate the resonant frequency, to know the effect of added dielectrics and to know the effect of gaps between the FSS and dielectric. There are several rules of thumb which give a good starting place for a design.

The first step is to estimate the resonant frequency for an FSS in free space. In this situation, a center connected element will resonate when each segment of the element is about a quarter of a wavelength from center to tip. Loop elements, on the other hand, will resonant when their average circumference is about a wavelength. Plates are more complicated, but a good first guess is that the plate should be about a half of wavelength across. Combination elements are too diverse to estimate the resonant frequency [2].

Dielectric added either to one or both sides of the FSS can affect the resonant frequency a noticeable amount when the dielectric is only $0.0167\lambda_0$ thick. Maximum reduction in the resonant frequency can be obtained when the dielectric is as thin as $0.05\lambda_0$. The resonant frequency of an FSS in a thick dielectric is reduced by a factor of $\sqrt{\varepsilon_r}$ when the dielectric is present on both sides of the dielectric and by a factor of $\sqrt{(\varepsilon_r+1)/2}$ when the dielectric is only present on one side of the dielectric. Note that these equations assume that the permeability in the dielectric is the same as the free space value, which is generally the case. ε_r is the relative permittivity of the material; this value is also known as the dielectric constant. When the dielectric is between about $0.0167\lambda_0$ and $0.05\lambda_0$ thick, a mathematically convenient factor known as the effective dielectric, ε_{eff}, is employed in lieu of ε_r. An example showing the trend of the variation of the relative permittivity of the medium the FSS for dipoles of various lengths is in is shown in Figure 2.6. In this figure, ε_{eff} is plotted as a function of the dielectric thickness. Since the dielectric is only on one side, ε_{eff} can vary between 1 and $\sqrt{(\varepsilon_r+1)/2}$. The thickness of the dielectric is given in mm. However, a thickness of about 1.5 mm corresponds to about $0.05\lambda_0$ for this example. Notice that longer wires require thicker dielectrics to have the same impact on the dielectric constant as compared to shorter wires.

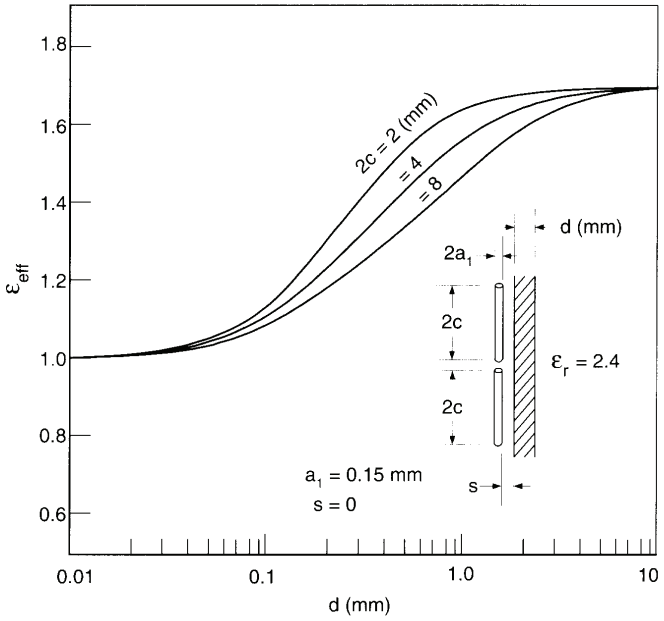

Figure 2.6: Variation of the effective dielectric constant as a function of dielectric substrate thickness and element length for dipole elements when the dielectric is added to one side. From [2].

Another significant parameter to consider is the effect of an air gap on the dielectric constant. A plot of the variation of dielectric constant as a function of air gap between the FSS and the dielectric is shown for two parallel wires between a dielectric in Figure 2.7. This shows that even small air cracks can have a large impart on the dielectric constant. In fact, air cracks as low as $0.0167\lambda_0$ (s=0.05 mm) can reduce the dielectric constant by about 5 percent. An air crack of about $0.1\lambda_0$ (s=3 mm) can reduce the effective dielectric constant to very nearly the free space value, even for thick dielectrics. This can be explained by the fact that the effective dielectric constant is determined by what percentage of the stored energy around the wires is stored in a given medium. Most of the reactive energy is stored near the element, so it is expected that even small air gaps can result in fairly significant changes in the effective dielectric constant.

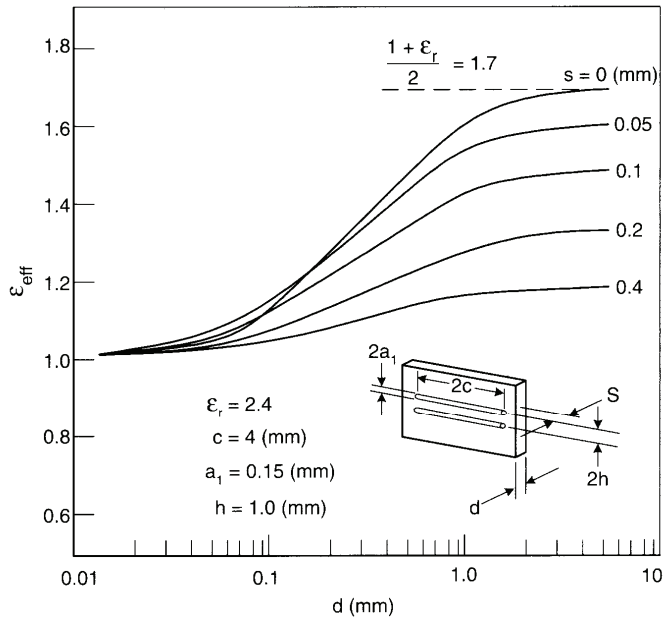

Figure 2.7: Effect of the spacing between the dielectric and the FSS as a function of substrate thickness. From [2].

This last fact points to the need to use printed circuit-type technology when constructing FSS arrays for the simple reason that even if the array was built with very tight tolerances between the FSS and the dielectric, the coefficients of thermal expansion are different for metals and dielectrics so air gaps would inevitably form over time [2].

2.2.4 Finite FSS Arrays

While infinite arrays are very useful for understanding many properties of FSS arrays, the only physically realizable arrays are finite. This fact introduces two major additional considerations to the design of an array, namely edge diffraction and radiating surface waves. Edge diffraction causes the stop band bandwidth to increase slightly.

Radiating surface waves show about 20-30 percent below resonance when the inter-element spacing is less than $0.5\lambda_0$. The array designed for this project resonates at a

frequency of about 1.425 GHz. Thus this array will expect to find surface waves somewhere between 1 to 1.14 GHz, which is the lower end of the operational band. In addition the presence of an radiating array changes the frequency range where surface waves will be found in the FSS ground plane [3]. As a result, surface waves may or may not be an issue for in project.

In frequency range where radiating surface waves exist, the finite array contains two surface waves which propagate along the array in opposite directions. The currents associated with these waves can be quite strong, many times stronger than the Floquet currents which are induced in both finite and infinite FSS arrays. They also travel with a different phase velocity than the Floquet currents, causing current fluctuations across the array. As a note, Floquet currents, are the currents induced by an incident wave used to excite the array and have the same amplitude and phase as the incident wave [3]. These surfaces waves cause particularly high currents near the edges of the array. The good news is that while the currents associated with surface waves are quite strong, they do not radiate as efficiently as Floquet currents. However, while these currents do not significantly affect the main beam, they can raise side lobe levels by 10 dB or more [3].

There are two main ways to reduce the presence of surface waves. The first is to curve the FSS, and the second is to add resistive loading to the elements to reduce the current levels. The addition of a resistive component to every element will lead to a significant degradation of the reflectivity of the FSS, unless the added resistance is small compared to the antenna impedance. Adding relatively small resistances can significantly reduce surface wave radiation while only reducing the reflectivity of the array by about 1 dB, making it a viable option. However, since the surface wave currents

are the highest at the edges, it is sufficient to only resistively load the edge elements with relatively higher resistances [3].

2.3 Radiating Element Theory

This section will briefly discuss a few possible alternatives for the radiating element array used to excite this antenna and methods to improve the bandwidth of the array. The three types of elements discussed are half wavelength dipoles, log-periodic antennas and dual rhombic loops. The advantages and disadvantages of each element type will be briefly presented.

The first type to consider is a crossed dipole. This element is advantageous because it is a simple element to construct. However this element is typically narrow-banded. In addition, if circular polarization is desired, two orthogonal dipoles which are 90 degrees out of phase which each other must be used [1].

A second type of antenna is a log-periodic antenna. This antenna is composed of a linear array of dipoles connected by a center spine which increase logarithmically in size and which are spaced in a logarithmic manner. As a result this antenna is capable of realizing relatively flat gain over a potentially large bandwidth, depending on the range of dipoles used [1]. Here again, if circular polarization is desired, two orthogonal antennas which have a relative phase delay of 90 degrees between them is necessary. As a side note a conical spiral, which more or less looks like a megaphone, is able to realize circular polarization over a bandwidth of 7 to 1 [1]. Unfortunately, this element is 3-D in nature. Since this project is attempting to minimize the space taken up by the arrays, this is not a good choice either.

A third option is known as a dual rhombic antenna. This antenna is capable of realizing circular polarization with a single input over a frequency range of up to 20%. As a result this element does not truly meet the definition of wide-band. There are two types of dual-rhombic antennas, as shown in bottom of Figure 2.8. One is a dipole type series feed, as shown in the bottom left figure. The second is a loop type parallel feed, as shown in the bottom right figure [4].

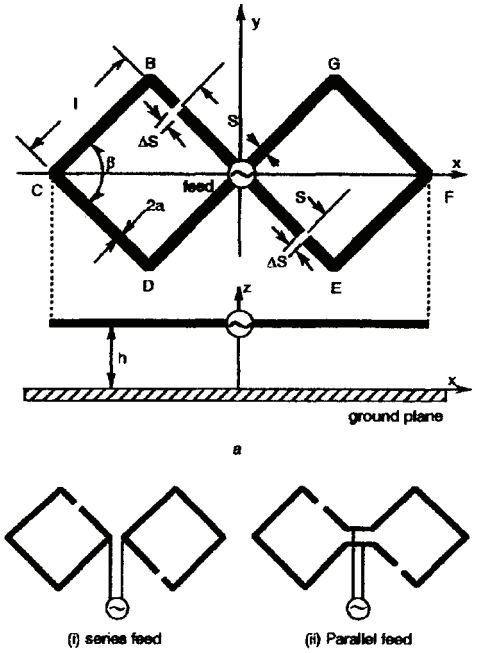

Figure 2.8: The two different types of dual rhombic loops. The one shown on the bottom left is a series fed loop. The one shown on the bottom right is a parallel feed loop. From [4].

There are three major ways to increase the bandwidth a radiating element array. The first method is to increase the wire radius and decrease the inter-element spacing. The second is to add a ground plane behind the radiating array. For this method to work, the radiating array must vary slowly and monotonically from capacitive to inductive over the entire frequency range. If an array circles between capacitive and inductive regions

of the Smith chart several times over the frequency range, the addition of the ground plane will instead hurt the bandwidth [3].

To accomplish this increase in bandwidth by adding a ground plane, an array whose reactance varies slowly from capacitive to inductive should be placed a quarter of a wavelength away from the ground plane at its resonant frequency. At this point, the real part of the ground plane impedance is zero since ground plane impedances are purely reactive and, at a quarter wavelength spacing, the array "sees" an infinite impedance at the ground plane [3]. This is in short explained by the fact that a wave will travel a half of a wavelength from the source to the ground plane and back to the source and will add 180 degree phase difference when it hits the ground plane. Starting from the θ=0 degrees point on the Smith chart ($jX_A = j\infty$), and rotating a half wavelength in the clockwise direction around the R=0 circle, this puts the impedance at $jX_A = j0$. However the ground plane adds a 180 degree phase shift, which brings the impedance back to $jX_A = j\infty$ [3]. At lower frequencies, the wave will not travel as far in terms of wavelengths from the source to the ground plane and back to the source so the resulting impedance will end up in the inductive reactance region of the Smith chart; in other words the ground plane "looks" like an inductor to the radiating array. Likewise when the spacing is larger than a quarter wavelength, the ground pane "appear" capacitive. The FSS array, however, can be approximated as a series inductor and capacitor. At frequencies below resonance, the array will become capacitive. As a result, the ground plane and array reactances will partially cancel each other out, bringing the overall impedance closer to the $jX_A = j\infty$ (close to the in phase condition) than if the ground plane wasn't there [3].

Another method to increase the bandwidth is to increase the real part of the ground plane impedance. One method to accomplish this is to add a material between the array and the ground plane which has a higher impedance than free space. Since a suitable material with a higher relative μ than relative ε does not exist, this method will not work. However, if a dielectric added in front of the array, this will lower the impedance in front of the array relative to the impedance behind the array. If the addition of the dielectric does not affect the ground plane impedance, then the ground plane impedance will be effectively increased [3]. Discussion of the theory behind the addition of dielectric substrates to improve radiating array bandwidth is beyond the scope of this paper. Consult [3] for a detailed derivation of the pertinent theory.

Chapter 3

Computer Simulations

3.1 Introduction

This project employed the use of ESP5, an industry standard Moment of Methods (MoM) code to design the antenna. This code was developed by Dr. Edward Newman at the ElectroScience Lab (ESL) at The Ohio State University [6]. The geometry files for the ESP5 runs were generated using MATLAB scripts. In addition the collected data was manipulated and plotted using MATLAB scripts.

The computer simulations were completed in several steps. The FSS and the array were designed independently and then combined together. The FSS was designed first. Tests were run to determine the L-band (stop band) reflectivity and the pass band transmissivity. Afterward the radiating array was designed. Tests were run to determine

L-band performance. Finally, the reflectivity and transmissivity of the FSS combined with the radiating array was tested.

Numerical limitations place several restrictions on the geometry. Two limitations in particular played a significant role in determining the overall geometry. These two limitations are the requirement that the wire radius not exceed 0.02λ at the analysis frequency and that wires need to be separated by several radii [6]. For the purpose of this project, the wires are separated by a minimum of 6 wire radii center to center to ensure reliable results. Good results are obtained in the L-band even with these restrictions in place. However, the thin wire limitation placed a very undesirable upper frequency limit of about 3680 MHz for the final design. The only way to get around this restriction is to use thinner wires. However thinner wires result in better transmissivity outside of the L-band so such simulations would have given better-than-best case scenario results.

The final geometry was also simulated in another code known as PMM [7], which was developed at ESL.[1] This code uses the periodic moment method, making it useful for simulating infinite geometries. Output from this code is useful in part as a comparison to the finite geometry results. In addition, PMM is able to simulate the geometry at much higher frequencies, giving a good idea what the transmissivity properties are at higher frequencies.

Also an important note on is that the results obtained in ESP5 are impedance matched every input at every frequency to obtain maximum gain [6]. As a result, the output generated by ESP5 is better than what will actually be obtained. Since the real part of the impedance does not vary significantly with frequency, this will not result in

[1] The author would like to thank Dr. Ronald Marhefka at ESL for running the simulations in PMM.

more than 1-2 dB of loss if the impedance used in the actual input impedance is around the average impedance. In addition the impedance does not vary significantly between elements, allowing the user to use the same input impedance for every element.

3.2 FSS Alone

The first part of this section will detail important FSS dimensions. Following this, plots of the L-band reflectivity and upper band transmissivity will be discussed. Finally these results will be compared to results obtained using PMM.

The FSS geometry is shown in Figure 3.1. The figure to the left shows the XY plane view of the geometry, and the figure to the right shows the YZ plane view. This geometry consists of two identical 3x6 FSS arrays composed of hexagonal elements. This array is designed to resonate at around 1.425 GHz. The segments of the hexagon are each 3.51 cm long. The element to element spacing (E2E) is 7.21 cm, the closest wire to wire spacing (W2W) is 1.14 cm, and the arrays are separated by 10.5 cm. The wire radius is 1.63 mm (8 AWG). The overall array dimensions are about 43.5 cm x 33.0 cm x 10.5 cm.

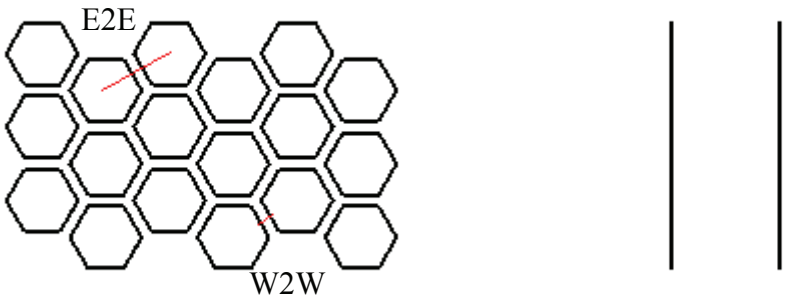

Figure 3.1: XY and YZ views of FSS geometry, which consists of two identical 3x6 FSS arrays composed of hexagonal elements. The element to element spacing (E2E) is 7.21 cm, the wire to wire separation is 1.14 cm and the arrays are separated by 10.5 cm. The wire radius is 1.63 mm (8 AWG) and the overall array dimensions are 43.5 cm x 33.0 cm.

The first test run was a reflectivity test at L-band. The geometries used can be seen in Figure 3.2. It is composed of two identical 8x16 hexagonal arrays. Two tests were run, which are detailed in the next paragraph. Figure 3.2(a) shows the XY plane view of the geometry. This view is more or less the same for both geometries. Figure 3.2(b) shows the XZ plane view of the first geometry, where a dipole is placed behind the FSS parallel to the x axis. Figure 3.2(c) shows the YZ plane view of the second geometry, where a dipole is placed behind the FSS parallel to the y axis. Two orthogonal dipole configurations are used in order to get complete information about the FSS transmissivity as a function of frequency.

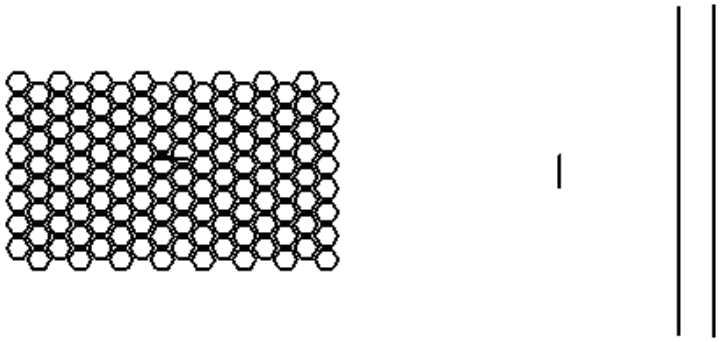

(a) (b)

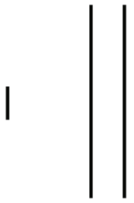

(c)

Figure 3.2: Plane view of the two geometries used to test the FSS reflectivity and transmissivity. Figure 3.2a shows the XY plane view, which is more or less the same for both geometries. Figure 3.2b shows the XZ plane view when a dipole is placed behind the FSS along the x axis, and Figure 3.2c shows the YZ plane view when a dipole is placed behind the FSS along the y axis.

The results for these tests are shown in Figure 3.3. This test was completed by placing a dipole parallel to the x axis in Figure 3.3(a) and parallel to the y axis in Figure 3.3(b) which is a half wavelength long at 1.425 GHz and 7/3 of a wavelength behind the closest FSS array. The transmissivity of this dipole through the FSS at boresite (along the positive z axis) was collected. The transmissivity data was then normalized to the

dipole's output without the array present and converted to the reflectivity data shown in Figure 3.3. As a result this data is normalized such that 0 dB corresponds to perfect reflectivity. As part of the transformation from transmissivity to reflectivity, all data points which had a transmissivity of 95 percent or more were set to 95 percent. This corresponds to a reflectivity of -13 dB. This was done to prevent the graph from going too far down so that the detail of the reflectivity performance was not lost in scaling. As these figures show, the FSS has a very flat gain curve (within a dB) over the entire L-band and relatively fast roll off on either edge of the stop band.

This procedure makes the assumption that the FSS is a lossless filter which does not affect the energy distribution and that no edge diffraction occurs. In reality a small percentage of the energy is diffracted around the FSS. The most noticeable effect of edge diffraction is the upper reflectivity null is shifted to the right and filled in a bit. However, since the phase variation with dipole spacing is significantly greater for the edge diffracted power components then the components which travel straight through the FSS, it is possible to average out edge diffraction by running several (4-5 should be sufficient) tests at slightly different spacing and average the resulting data together. Due to time constraints, this test was not completed.

In addition an FSS is not an ideal filter since it will redistribute energy in different directions. As a result, it is possible for more energy to be measured a given location than was transmitted by the dipole. The first few data points of every run showed higher than unity transmissivity, which can be seen in Figure 3.4.

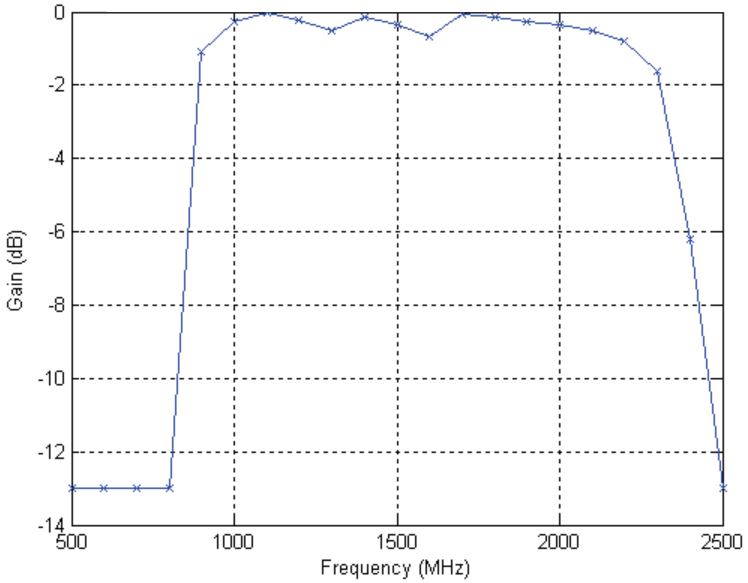

(a)

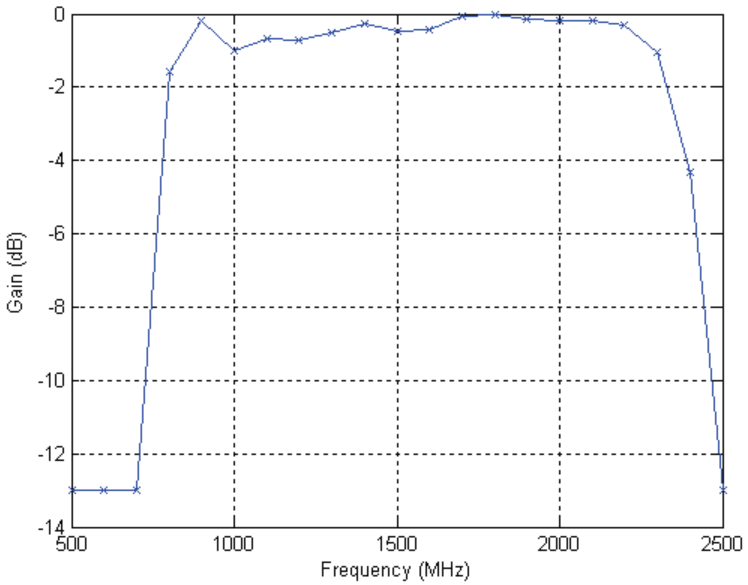

(b)

Figure 3.3: Reflectivity of an FSS composed of two arrays of regular hexagonal elements which were designed to resonate at 1.425 GHz. The center to center spacing of two nearest neighbor elements is 7.21 cm and the arrays are separated by 10.5 cm. The wire radius is 1.63 mm. (a) The dipole is parallel to the x axis (b) The dipole is parallel to the y axis.

Next the transmissivity of this array is shown in Figure 3.4. These tests use the same geometry shown in Figure 3.2. Here again, Figure 3.4(a) is the results when the dipole is aligned parallel to the x axis and Figure 3.4(b) shows the results when the dipole is aligned parallel to they y axis. As was noted earlier, ESP5 can only compute results up to a frequency of about 3.68 GHz at the wire radius used. The only way to simulate higher frequencies would be to reduce the wire radius, which would generate better-than-best case scenario results.

These results show that there is a significant amount of energy redistribution from about 500-700 MHz. The dip in transmissivity from 2500-3500 MHz is perhaps a filter ringing effect type dip. This transmissivity dip has been seen in other similar projects and so is not unexpected. As the PMM data will show later, the overall transmissivity improves significantly after this point. Figure 3.4(b) likely does not show as much of a transmissivity dip as Figure 3.4(a) due to higher levels of edge diffraction.

As has been stated earlier, the purpose of looking at transmissivity is the intent to place a second antenna behind this one operating in a band above L-band and have it be able to "look through" this band without a significant level of attenuation or scattering. Since it is not possible to test these higher frequency bands using ESP5, it is not possible to design a dielectric matching section to improve transmissivity. If improving transmissivity at higher bands is desired, it will be necessary to employ the use of a different computer program.

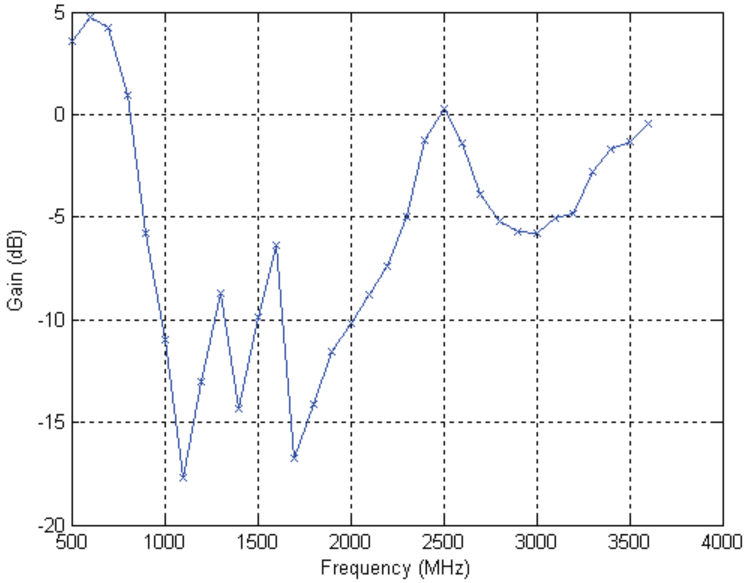

(a)

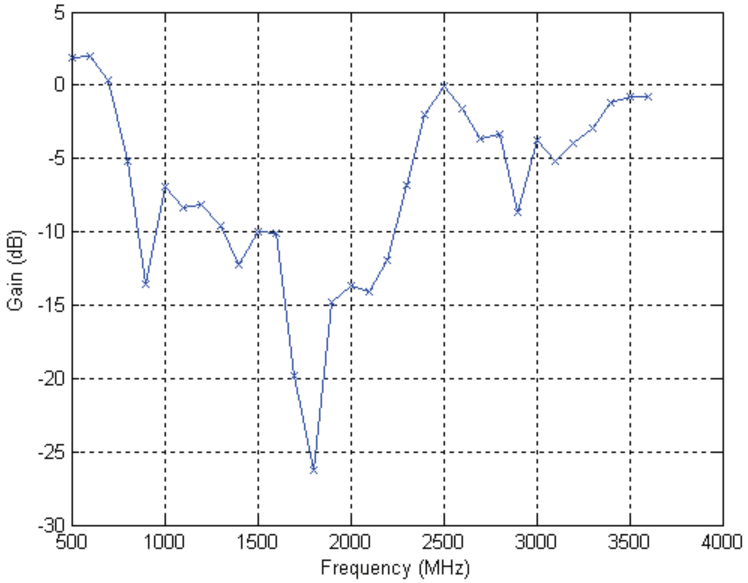

(b)

Figure 3.4: Transmissivity of an FSS composed of two arrays of regular hexagonal elements which were designed to resonate at 1.425 GHz. The center to center spacing of two nearest neighbor elements is 7.21 cm and the arrays are separated by 10.5 cm. The wire radius is 1.63 mm. (a) The dipole is parallel to the x axis (b) The dipole is parallel to the y axis.

In addition to testing the FSS using ESP5, the FSS was also tested using PMM. PMM calculates the reflectivity and transmissivity of an infinite array which is excited by an incident plane wave. As a result, these results do not have edge diffraction or energy redistribution effects added in. The PMM tests were run from a frequency of 500-8500 MHz with a step of 250 MHz. Figure 3.5 shows the reflectivity of two FSS arrays, similar to the ones shown in Figure 3.2 expect that these arrays are infinite.

Notice in Figure 3.5 that the reflectivity is very good from about 1-1.5 GHz. The strong null seen at 1.75 GHz is the same null seen around 2.5 GHz in Figure 3.7. As was explained earlier, this null is expected to shift to higher frequencies for the finite array case due to edge diffraction effects. In addition, a mode which is trapped between the two FSS arrays occurs at about 3.65 GHz and a grating lobe occurs at about 5.4 GHz. Grating lobes and trapped modes cannot be avoided; they can only be shifted in frequency by changing the spacing between the arrays in the case of the trapped mode and changing the inter-element spacing in the case of the grating lobe.

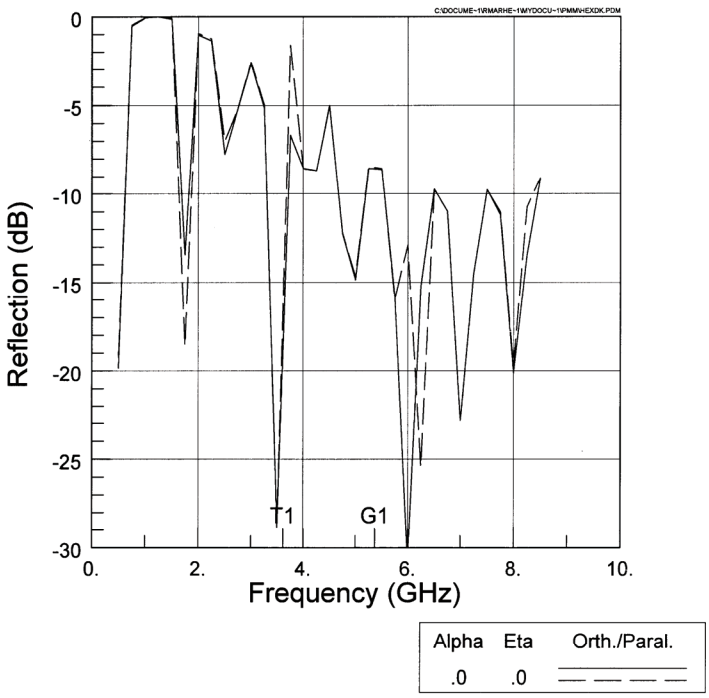

Figure 3.5: Reflectivity of a two layer infinite FSS composed of hexagonal elements which is designed to be reflective in the L-band.

Figure 3.6 shows the transmissivity of the same geometry. Notice that after the huge dip in transmissivity around 1.6 GHz, there is another dip which is about 100 MHz wide. This is the same dip at the one seen from 2.5-3.5 GHz in Figure 3.3. Notice that above this frequency, the transmissivity of the array is significantly better. Based on these results, C band (4-8 GHz) would likely make a good choice for an antenna to operate at behind this one.

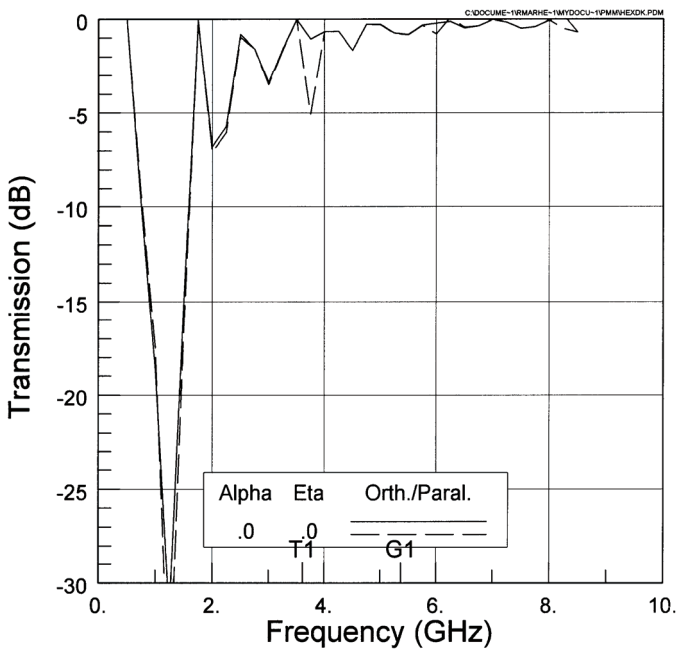

Figure 3.6: Transmissivity of a two layer infinite FSS composed of hexagonal elements which is designed to be reflective in the L-band.

3.3 Radiating Array Alone

Upon completing the design and testing of the FSS ground plane, the same process was completed for the radiating array. The geometry for the radiating array is shown in Figure 3.7. This array is composed of four series fed dual rhombic antennas which are designed at 1750 MHz. These elements are spaced 15.4 cm in the x direction ($0.9\lambda_0$) and 8.57 cm ($0.5\lambda_0$) in the y direction. In addition the elements are rotated clockwise by 15 degrees and have had their ends cut off in order to allow for closer spacing of the elements.

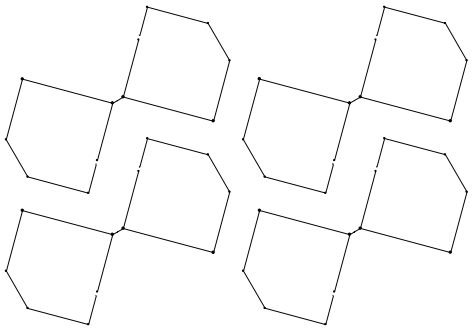

Figure 3.7: This figure shows the radiating array geometry used in this project. This array consists of four series fed dual rhombic loop antennas which are designed at 1750 MHz. The elements are rotated 15 degrees in the clockwise direction and have their ends cut off to allow for closer spacing. These elements are spaced 15.4 cm in the x direction ($0.9\lambda_0$) and 8.57 cm ($0.5\lambda_0$) in the y direction.

After a few trials with various radiating element spacing, it was decided to space the array 3.75 cm ($0.125\lambda_{1GHz}$ or $0.25\lambda_{2GHz}$) above the ground plane. This decision was made primarily because this spacing resulted in the flattest gain curve when the PEC plate ground plane was replaced with the FSS ground plane. This will be explained in more detail in the next section. The gain of this antenna is shown in Figure 3.8.

Originally the intention was to design a circularly polarized wide-band radiating array. However, the bandwidth of circular polarization was not sufficient and time constraints prevented the attempt to improve the circular polarization bandwidth. As Figure 3.8 shows, however, the gain received by a linear antenna oriented parallel to the x axis (Gth) is reasonably flat.

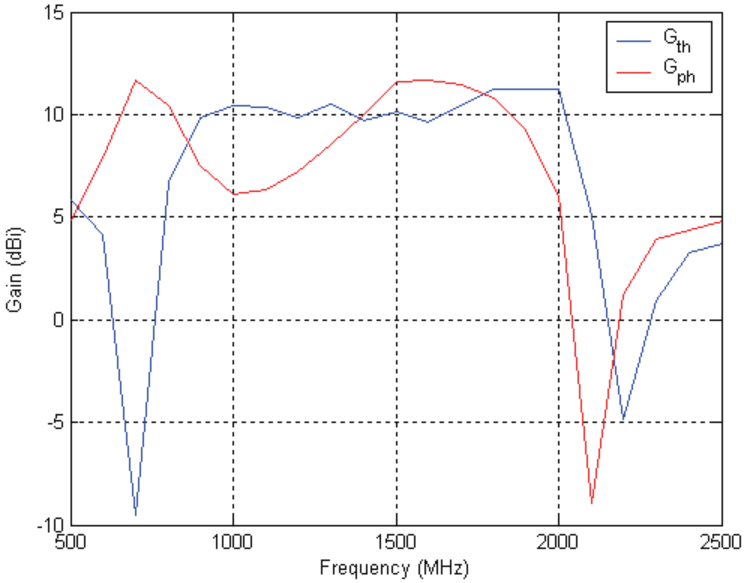

Figure 3.8: Plot of linear gain of a four element dual rhombic antenna array. This array is placed 3.75 cm ($0.125\lambda_{1GHz}$ or $0.25\lambda_{2GHz}$) above a PEC ground plane.

As was noted earlier, the gain seen here is impedance matched. The input impedance for one of the feeds is shown in Table 3.1. Note that each feed has roughly the same input impedance. This table indicates that feeding the elements with a 100 Ω coaxial cable will provide sufficient matching over the entire frequency range.

Table 3.1: This table shows input impedance of the radiating element feeds as a function of frequency. The impedance for one feed is shown here; however, each feed has roughly the same input impedance as a function of frequency.

Freq (MHz)	R	jX
1000	113.40	-75.83
1100	72.24	-66.92
1200	43.71	-33.75
1300	145.40	-18.69
1400	128.40	-28.68
1500	99.21	-40.19
1600	68.02	-25.91
1700	75.50	11.44
1800	98.64	14.60
1900	105.70	21.03
2000	124.10	18.94

3.4 FSS and Radiating Array Combined

After the array and the FSS were designed, the last step remaining in the design process was to simulate the FSS and array together. The FSS array size and the FSS to radiating element spacing was determined using this geometry. The final geometry is shown in Figure 3.9. Figure 3.9(a) shows the XY plane view and Figure 3.9(b) shows the YZ plane view of the geometry. The FSS is identical to the one shown in Figure 3.4 and the radiating array is the same one shown in Figure 3.7.

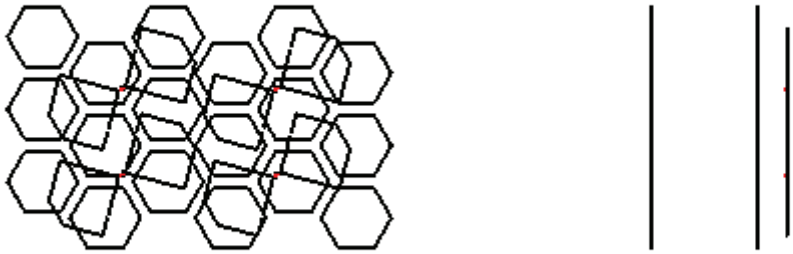

(a) (b)

Figure 3.9: The final geometry for the FSS and radiating array. Figure 3.9(a) shows the XY plane view and Figure 3.9(b) shows the YZ plane view of the geometry.

The reflectivity of this array over L-band is shown in Figure 3.10. This geometry was chosen since it produced the flattest gain curve over L-band. A smaller array could not be used since it would be too small for the radiating array. Larger arrays resulted in flatter gain in the upper half of the L-band at the expense of a relatively large bump and dip in the gain at the lower half. Also spacing the radiating array farther from the FSS resulted in flatter gain at the lower half of the band at the expense of a significant gain dip

from 1900-2000 MHz. This gain dip is due to the fact that the spacing at these higher frequencies was getting too close to λ/2, a spacing which causes a large null in the gain since the transmitted and reflected fields are 180 degrees out of phase with each other.

As is shown in Figure 3.10, the L-band gain for this geometry varies by 3 dB over the range of interest. The other array configurations, while they had a higher average gain by about a dB, produced larger fluctuations in gain.

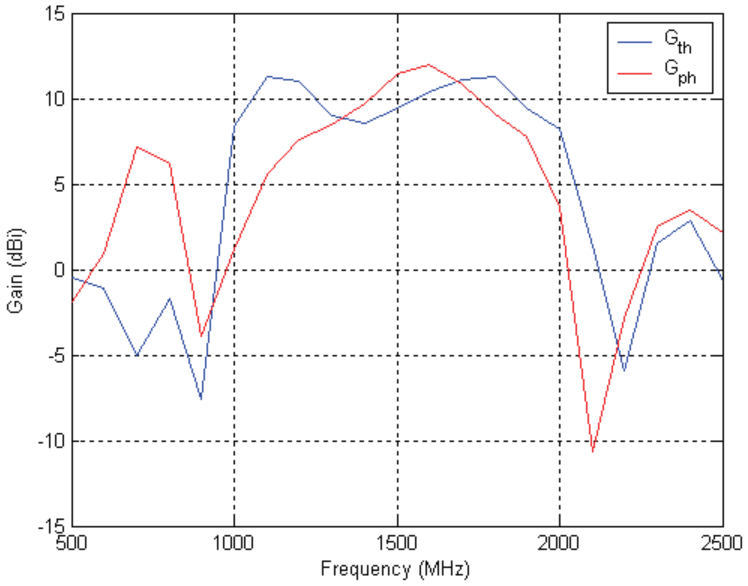

Figure 3.10: This figure shows the output for the final array geometry. This geometry is composed of two identical 3x6 arrays separated by a half wavelength at the design frequency of 1.425 GHz and is composed of hexagonal elements. The radiating array is composed of four series fed dual rhombic loops which have their tips cut off. This geometry resulted in the flattest gain curve, with a variation of 3 dB over the L-band.

Figure 3.11 shows the results of the transmissivity tests completed for this geometry. This test was completed by placing a dipole behind the FSS and turning off the dual rhombic elements. Two 8x16 FSS arrays with a 3x6 dual rhombic loop array was used to minimize edge diffraction and to keep the test as consistent as possible with earlier FSS transmissivity tests. Figure 3.11(a) shows the results when the dipole is

placed parallel to the x axis and Figure 3.11(b) shows the results when the dipole is placed parallel to the y axis. The resulting data was then normalized to the dipole gain at each frequency. The major difference between Figure 3.11(a) and Figure 3.7(a) is the transmissivity dip from 2500-3600 MHz has been shifted to the left a bit. Figure 3.11(b) shows improved transmissivity as compared to Figure 3.7(b) in 2500-3600 MHz frequency range. As a result, adding the array improved the transmissivity in this range. This is mostly of academic interest since an antenna placed behind this one will not be operating in this frequency range. This improvement in transmissivity is likely due to coupling between the FSS and the radiating array.

It is interesting to note that when the radiating array was placed 5.3 cm instead of 3.75 cm ($0.25\lambda_{1.425GHz}$ vs. $0.125\lambda_{1GHz} = 0.178\lambda_{1.425GHz}$) from the top FSS, the gain dip from 2500-3500 MHz becomes about 2.5 dB deeper than when the radiating array is not there.

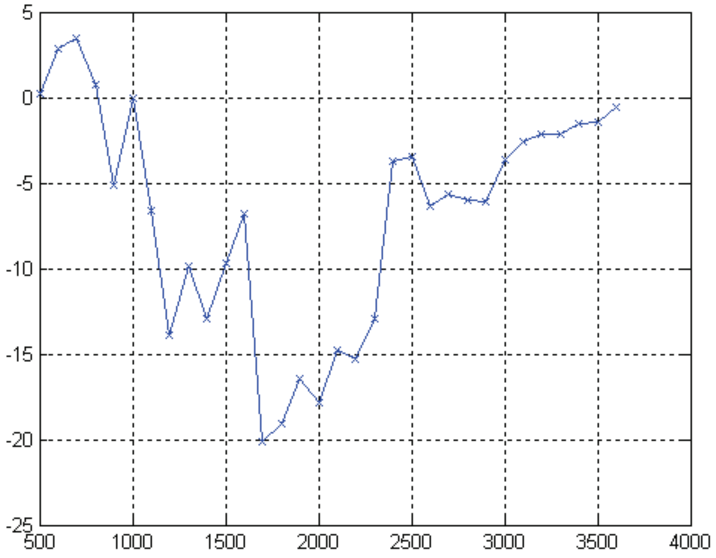

(a)

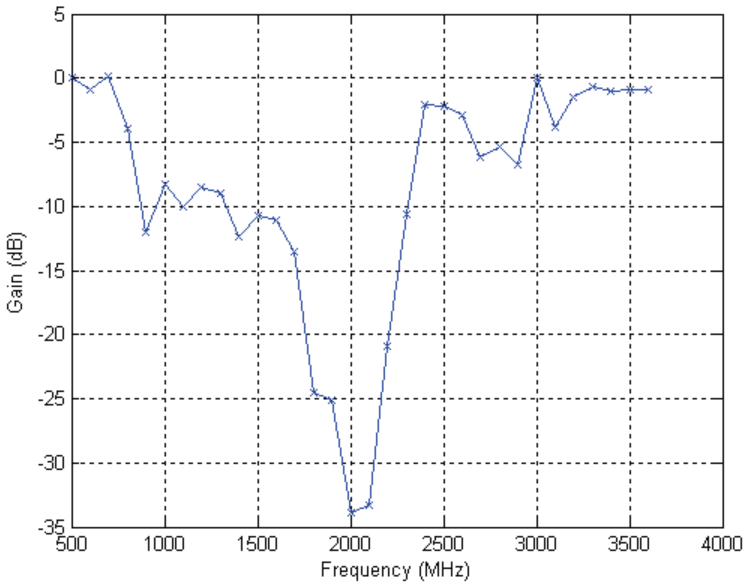

(b)

Figure 3.11: The figures above show the transmissivity of a dipole through the final FSS and dual rhombic array geometry. Figure 3.10a shows the transmissivity when the dipole is placed parallel to the x axis, and Figure 3.10b shows the transmissivity when the dipole is placed parallel to the y axis. The addition of the radiating array improves the overall transmissivity of the antenna, as compared to the transmissivity of the FSS alone. This is likely attributed to coupling between the dual rhombic array and the FSS.

Finally tests were run to determine if surface waves were present around 1 GHz. These tests were run by computing volumetric cuts of the antenna over a range of frequencies. The resulting output indicates that surfaces waves are not present at the lower end of the L band. This is likely due to the relatively high level of coupling occurring between the FSS and the radiating array which is altering the characteristics of the FSS. This coupling will be reduced for larger array spacing, but at the expense of reduced gain at the upper L band frequencies. Time constraints prevented the testing for the presence of surface waves if the FSS to radiating array spacing was increased. As a result, it is not conclusively known if coupling is the reason for the lack of surface waves at the lower end of the frequency range.

Chapter 4

Prototype Build and Test

4.1 Prototype Build

After designing the antenna using ESP5, the next step was to build and test a prototype. Due to time constraints, only a prototype of the FSS reflector was built and tested. Since the design of the FSS was the main goal of this project, this is a suitable substitution. This prototype was constructed using 8 gauge wire (AWG), which is the wire radius the antenna was designed for. The wire has a polyethylene coating which is about 0.75 mm thick and a very thin nylon coating on top of that. The array was constructed by taping the elements to a piece of Styrofoam using standard masking tape. The Styrofoam has a very low dielectric constant, so it does not noticeably affect the results.

4.2 Prototype Test

This array was tested by hooking up a 1-12 GHz horn antenna to each port of the network analyzer. The FSS was placed between these two horn antennas and S21 measurements were obtained over the desired frequency. This measurement computes the transmissivity of the array. Where necessary, these results were mathematically transformed to reflectivity results, again using the assumption that the transmitted plus the reflected signal is equal to unity. Over the range of these tests, this is a good approximation.

Two separate tests were run. The first test was to measure the transmissivity of each array alone, and the second test measured the transmissivity of the two arrays together. The results of the first test are shown in Figure 4.1. Figure 4.1(a) and Figure 4.1(b) show the reflectivity of array 1 and array 2 respectively. This figure shows that the arrays are very similar to each other and that the resonance of this array is at about 1.2 GHz, instead of the design frequency of 1.4 GHz. PMM tests of a single array indicate that the resonance should have occurred around 1.4 GHz. This reduction in the resonant frequency is likely predominately due to the dielectric coating around the wires.

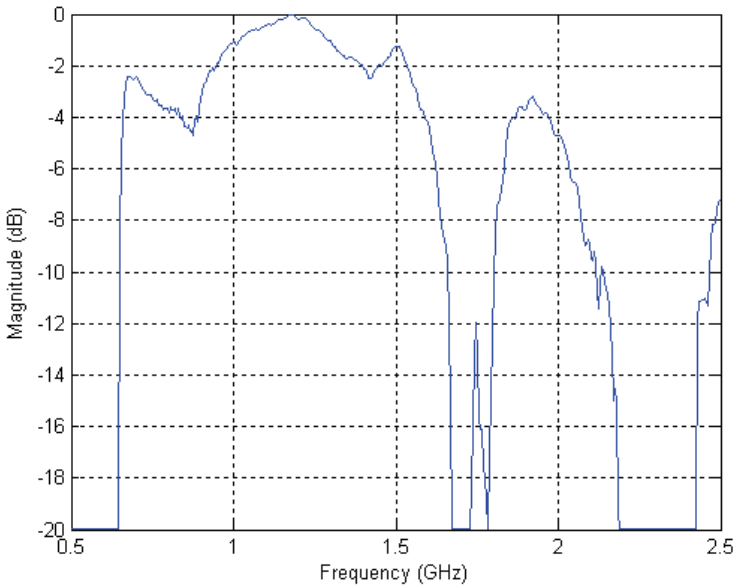

(a)

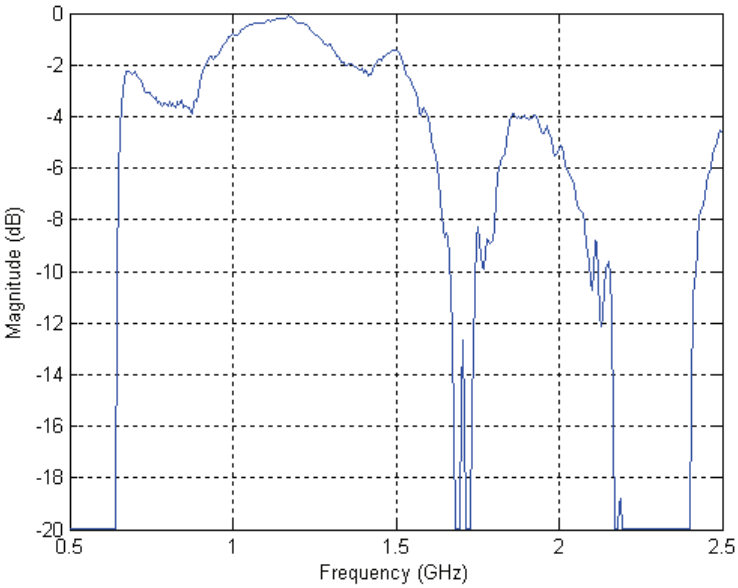

(b)

Figure 4.1: Reflectivity of (a) array 1 and (b) array 2. This figure shows that the arrays are very similar to each other and has a perfect resonance around 1.2 GHz instead of the design 1.425 GHz. This is likely due to the dielectric around the wires.

Next the reflectivity of the two arrays is shown in Figure 4.2. This curve shows that the array is within 2 dB of perfect reflectivity over L band. These results are very consistent with the results computed by ESP5. The reflectivity of the prototype is not quite as good as the computational results due to unavoidable imperfections in the construction of the prototype.

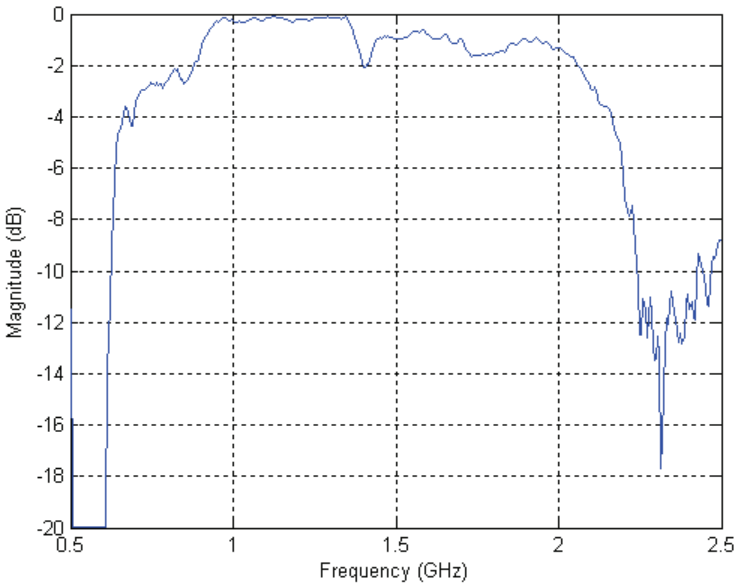

Figure 4.2: Reflectivity curve of the prototype FSS reflector.

An S21 measurement of the two arrays was then completed over a range of 1-12 GHz to determine the transmissivity of the array. These results are shown in Figure 4.3. This figure shows that the upper frequency transmissivity is quite poor. However, the transmissivity in the 1-2 GHz range is significantly different from results obtained in the shorter range runs that were used to determine the reflectivity in Figure 4.2. As a result, the results shown in Figure 4.3 are not trustworthy. Due to time constraints and equipment availability, it was not possible to rerun this test.

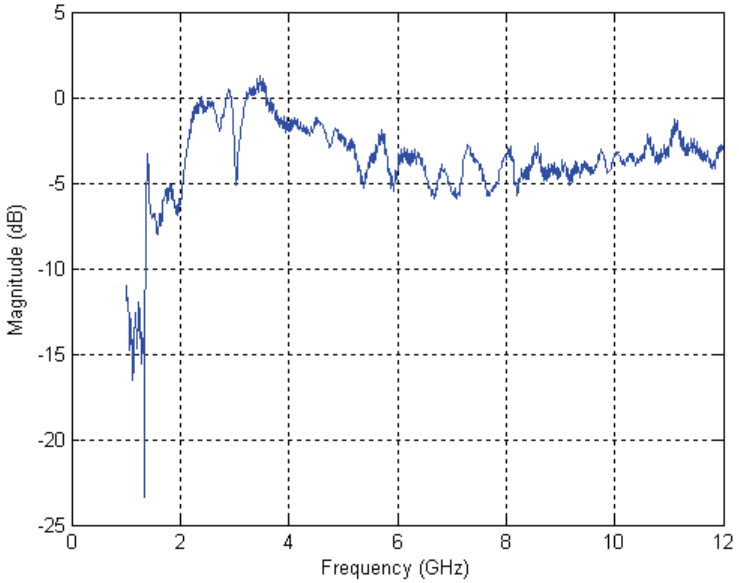

Figure 4.3: Transmissivity of the prototype FSS reflector. These results at lower frequencies are not consistent with other test runs at those frequencies. This indicates that the test results are not trustworthy.

Chapter 5

Summary and Conclusions

5.1 Summary and Conclusions

The purpose of this project was to construct a wide-band antenna which is transmissive outside of the band of operation. This type of antenna design would allow one or more antennas placed behind this antenna to "look through" it. This would allow for a greater density of antennas in places where the real estate upon which to place antennas is limited, such as on submarines and ships.

This antenna consists of a radiating element array in front of an FSS reflector. This FSS acts like a ground plane over the design band of 1-2 GHz (L-band) and is relatively transmissive sufficiently above this band. For this particular design, very good transmissivity is achieved, for example, from 4-8 GHz (C-band).

The FSS is composed of two identical 3x6 arrays of hexagonal elements, which are spaced a half wavelength apart at the design frequency of 1.425 GHz. The hexagonal

element was chosen due to its superior element bandwidth and close stacking potential. The radiating array is composed of four series feed dual rhombic loop elements which have their tips cut off to allow for close spacing. This radiating array is spaced $0.25\lambda_{2GHz}$ from the upper FSS array.

Transmissivity and reflectivity tests were completed for the FSS alone and the entire antenna. These results showed very good L-band reflectivity and very good transmissivity above about 3.5 GHz.

A prototype of the FSS was built and tested. The L band reflectivity of the FSS is consistent with previous results. The pass band transmissivity is inconsistent with computation results, however the data collected as part of this test is inconsistent with other prototype results. As a result, this data is not trustworthy.

References

[1] John D. Kraus and Ronald J. Marhefka, *Antennas: For All Applications*, 3rd ed. (New York: McGraw-Hill, 2002.)

[2] Ben A. Munk, *Frequency Selective Surfaces: Theory and Design*, 1st ed. (New York: John Wiley & Sons, Inc., 2000.)

[3] Ben A. Munk, *Finite Antenna Arrays and FSS*, 1st ed. (New York: John Wiley & Sons, Inc., 2003.)

[4] H. Morshita, K. Hirasawa, T. Nagao, "Circularly polarized wire antenna with a dual rhombic loop", IEEE Proc-Microw Antennas Propag., vol. 145, pp. 219-224, 1998.

[5] Fawwaz T. Ulaby, *Fundamentals of Applied Electromagnetics*, 3rd ed., (New Jersey: Prentice Hill, 2001.)

[6] E. H. Newman, *A User's Manual for The Electromagnetic Surface Patch Code: Release Version ESP5.3*, 2004.

[7] L. W. Henderson, "Introduction to PMM," Tech. Rept. 715582-5, Ohio State Univ., ElectroScience Lab, Dept. of Electrical Eng., prepared under contract F33615-83-C-1013 for the Air Force Avionics Lab., Air Force Wright Aeronautical Labs., Air Force Systems Command, Wright-Patterson Air Force Base, OH 45433, Feb. 1986.